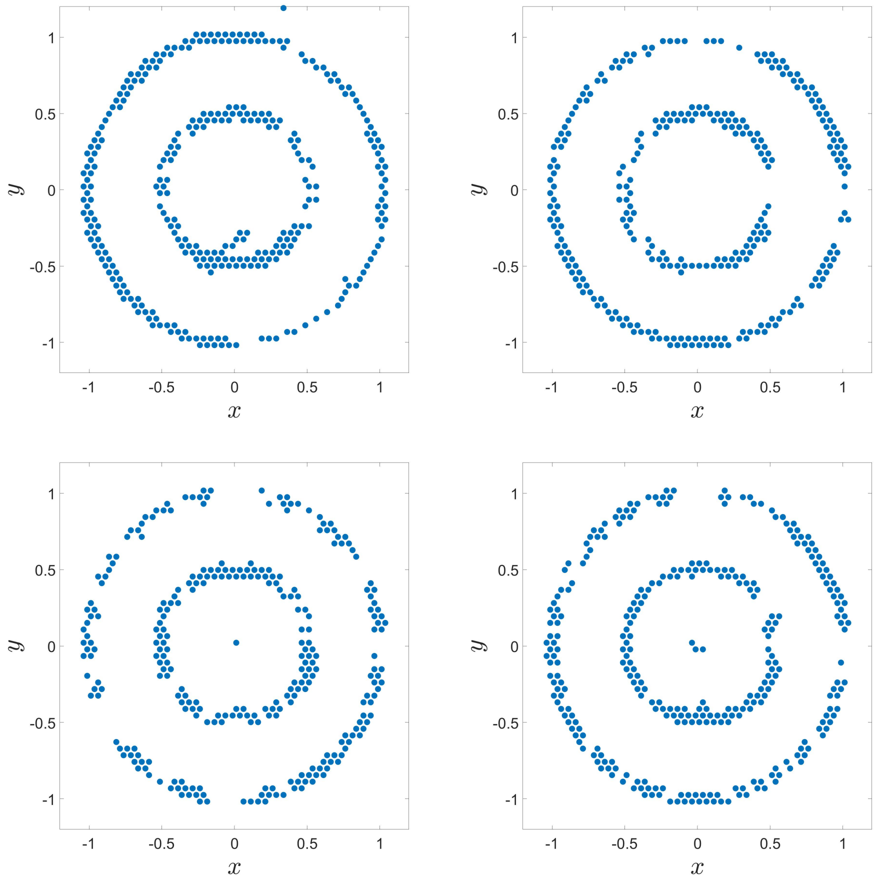

Figure 8: The area where β_i corresponding to the collocation point x_i fulfills $\beta_i \leq -10^{-5}$. $\dot{v}(x) = -1$ for $x \in I$ and $v(x) \leq 0$ for $x \in X \setminus I$ (upper left), $\dot{v}(x) = -1$ for $x \in M$ and $v(x) \leq 0$ for $x \in X \setminus M$ (upper right), $\dot{v}(x) = -1$ for $x \in O$ and $v(x) \leq 0$ for $x \in X \setminus O$ (lower left), and $\dot{v}(x) = -1$ for $x \in I \cup M \cup O$ and $v(x) \leq 0$ for $x \in X \setminus (I \cup M \cup O)$ (lower right).

points from the inequality constraint $\dot{v}(x_i) \leq 0$ to the equality constraint $\dot{v}(x_i) = -1$ if the value of β_i is close to zero, which indicates that $\dot{v}(x_i) < 0$ holds. We have used the criterion $\beta_i > -10^{-9}$ to ensure $\beta_i \approx 0$. However, we use the condition $\beta_i \leq -10^{-5}$ when plotting the chain-recurrent set to ensure $\beta_i \neq 0$.

In Figure 10 we depict the computed CLF candidate together with its orbital derivative $\dot{v}$ in the second step. The outcome is very similar, irrespective of which of the sets Γ we started with. This is very reassuring as it shows that the initial guess of Γ does not matter much and distinguishes very well between gradient-flow part and chain-recurrent set; by setting the orbital derivative to -1 in the numerically found gradient-flow part, the

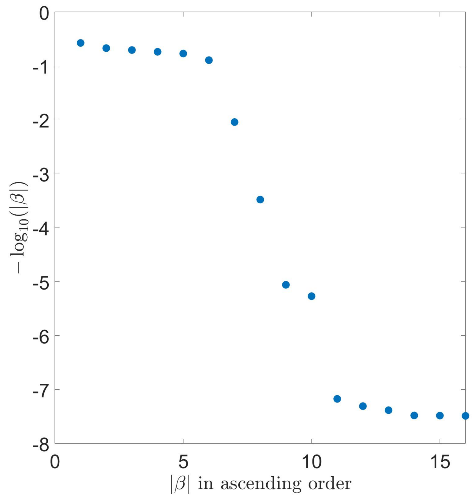

Figure 9: Ordering the coefficients $|\beta_i|$ in decreasing order and plotting $\log_{10}(|\beta|)$ gives the following result for points 320 to 335; this shows that there is a sharp decline between points close to zero and negative points.

values of the orbital derivative, and thus of the function itself, are not too small. Figure 11 displays the approximation to the chain-recurrent set of this second step using the CPA approximation to check where the derivative is strictly negative.

4.2 Three-dimensional example

In this section, we consider the three-dimensional system from [13, Section 5.3]

$$\begin{pmatrix} \dot{x} \\ \dot{y} \\ \dot{z} \end{pmatrix} = \begin{pmatrix} x(1-x^2-y^2) - y + 0.1yz \\ y(1-x^2-y^2) + x \\ -z + xy \end{pmatrix} = f(x, y, z). \tag{29}$$

In this example, the origin is an unstable equilibrium and there exists an asymptotically stable periodic orbit. On the set $\Gamma := [-0.1, 0.1] \times [0.75, 0.85] \times [-0.1, 0.1]$ we set $\dot{v}(x) = -1$, and we use the hexagonal grid as the collocation grid X in $\Omega = [-1.25, 1.25]^2 \times [-0.45, 0.45] \cap (B_{1.25} \setminus B_{0.75})$ and $c = 1$. We use different fineness parameters α to investigate the influence of the number of collocation points on the quality of the estimate of the chain-recurrent set, namely $\alpha = 0.18$, $\alpha = 0.12$, and $\alpha = 0.08$.

We estimate the chain-recurrent set again, using two different strategies. We first estimate the set where we cannot prove that the orbital derivative is negative. To estimate this set we triangulate the area $[-1.25, 1.25]^2 \times [-0.45, 0.45]$ into small simplices, more exactly we triangulate the area into $6 \cdot 1000^2 \cdot 400 = 2.4 \cdot 10^9$ tetrahedra equal in size, and then interpolate the computed CLF by a CPA CLF and check the conditions. We established in the first example that the approximation is considerably better in the second step and therefore we do not show the results for the first step here.

For $\alpha = 0.18$, $\alpha = 0.12$, and $\alpha = 0.08$, respectively, we show in Figures 12, 13, and 14 the area in Ω where $\dot{v}(x) < 0$ fails by using the CPA interpolation (top) and the collocation points where $\beta_i < 0$ (bottom), which correspond, using KKT conditions, to the chain-recurrent set, if we assume that the function converges to a CLF. The figures show that the approximation of the chain-recurrent set improves considerably as we increase the density of the collocation points.

5 Conclusions

In this paper we have considered a minimization problem with inequality and equality constraints for a general linear operator in a reproducing kernel Hilbert space. When discretized, the problem can be solved using quadratic programming. We have exploited the KKT conditions in this context and have shown strong convergence of the solutions of the discretized problems to the solution of the original problem.

We have then applied the general method to compute complete Lyapunov function candidates for dynamical systems and have presented examples which show that the method is able to identify the chain-recurrent set well.

References

[1] C. Argáez, P. Giesl, and S. Hafstein. Analysing dynamical systems towards computing complete Lyapunov functions. In Proceedings of the 7th International Conference on Simulation and Modeling Methodologies, Technologies and Applications, Madrid, Spain, pages 323–330, 2017.

[2] C. Argáez, P. Giesl, and S. Hafstein. Computational approach for complete Lyapunov functions. In Dynamical Systems in Theoretical Perspective. Springer Proceedings in Mathematics & Statistics. ed. Awrejcewicz J. (eds)., volume 248, pages 1–11, 2018.

[3] C. Argáez, P. Giesl, and S. Hafstein. Iterative construction of complete Lyapunov functions: Analysis of algorithm efficiency. In Obaidat, Ören, and D. Rango, editors, Simulation and Modeling Methodologies, Technologies and Applications, volume 947 of Advances in Intelligent Systems and Computing, pages 83–100. Springer, 2020.

[4] J. Auslander. Generalized recurrence in dynamical systems. Contr. to Diff. Equ., 3:65–74, 1964.

[5] H. Ban and W. Kalies. A computational approach to Conley's decomposition theorem. J. Comput. Nonlinear Dynam, 1(4):312–319, 2006.

[6] P. Bernhard and S. Suhr. Lyapounov functions of closed cone fields: From Conley theory to time functions. Commun. Math. Phys., 359:467–498, 2018.

[7] J. Björnsson, P. Giesl, S. Hafstein, C. Kellett, and H. Li. Computation of Lyapunov functions for systems with multiple attractors. Discrete Contin. Dyn. Syst. Ser. A, 35(9):4019–4039, 2015.

[8] S. Boyd and L. Vandenberghe. Convex Optimization. Cambridge University Press, 2004.

[9] C. Conley. Isolated Invariant Sets and the Morse Index. CBMS Regional Conference Series no. 38. American Mathematical Society, 1978.

[10] M. Dellnitz, G. Froyland, and O. Junge. The algorithms behind GAIO – set oriented numerical methods for dynamical systems. In Ergodic theory, analysis, and efficient simulation of dynamical systems, pages 145–174, 805–807. Springer, Berlin, 2001.

[11] M. Dellnitz, O. Junge, M. Rump, and R. Strzodka. The computation of an unstable invariant set inside a cylinder containing a knotted flow. In B. Fiedler, K. Groger, and J. Sprekels, editors, Equadiff 99 - Proceedings of the International Conference on Differential Equations, volume 2, pages 1015–1020. World Scientific, 2000.

[12] P. Giesl. Construction of Global Lyapunov Functions Using Radial Basis Functions. Lecture Notes in Math. 1904, Springer, 2007.

[13] P. Giesl. Computation of a contraction metric for a periodic orbit using meshfree collocation. SIAM J. Appl. Dyn. Syst., 18(3):1536–1564, 2019.

[14] P. Giesl, C. Argáez, S. Hafstein, and H. Wendland. Construction of a complete Lyapunov function using quadratic programming. In Proceedings of the 15th International Conference on Informatics in Control, Automation and Robotics, volume 1, pages 560–568, 2018.

[15] P. Giesl, C. Argáez, S. Hafstein, and H. Wendland. Minimization with differential inequality constraints applied to complete Lyapunov functions. Math. Comp., 90:2137–2160, 2021.

[16] P. Giesl and S. Hafstein. Computation and verification of Lyapunov functions. SIAM J. Appl. Dyn. Syst., 14(4):1663–1698, 2015.

[17] P. Giesl, S. Hafstein, and S. Suhr. Existence of complete Lyapunov functions with prescribed orbital derivative. Discrete Contin. Dyn. Syst. Ser. B, 11(20):6927–6941, 2022.

[18] P. Giesl and H. Wendland. Meshless collocation: error estimates with application to Dynamical Systems. SIAM J. Numer. Anal., 45(4):1723–1741, 2007.

[19] A. Goullet, S. Harker, K. Mischaikow, W. Kalies, and D. Kasti. Efficient computation of Lyapunov functions for Morse decompositions. Discrete Contin. Dyn. Syst. - Series B, 20(8):2419–2451, 2015.

[20] A. Goullet, S. Harker, K. Mischaikow, W. D. Kalies, and D. Kasti. Efficient computation of lyapunov functions for morse decompositions. Discrete and Continuous Dynamical Systems - B, 20(8):2419–2451, 2015.

[21] M. Hurley. Noncompact chain recurrence and attraction. Proc. Amer. Math. Soc., 115:1139–1148, 1992.

[22] M. Hurley. Chain recurrence, semiflows, and gradients. J. Dyn. Diff. Equat., 7(3):437–456, 1995.

[23] M. Hurley. Lyapunov functions and attractors in arbitrary metric spaces. Proc. Amer. Math. Soc., 126:245–256, 1998.

[24] W. Kalies, K. Mischaikow, and R. VanderVorst. An algorithmic approach to chain recurrence. Found. Comput. Math, 5(4):409–449, 2005.

[25] H. Wendland. Scattered data approximation, volume 17 of Cambridge Monographs on Applied and Computational Mathematics. Cambridge University Press, Cambridge, 2005.

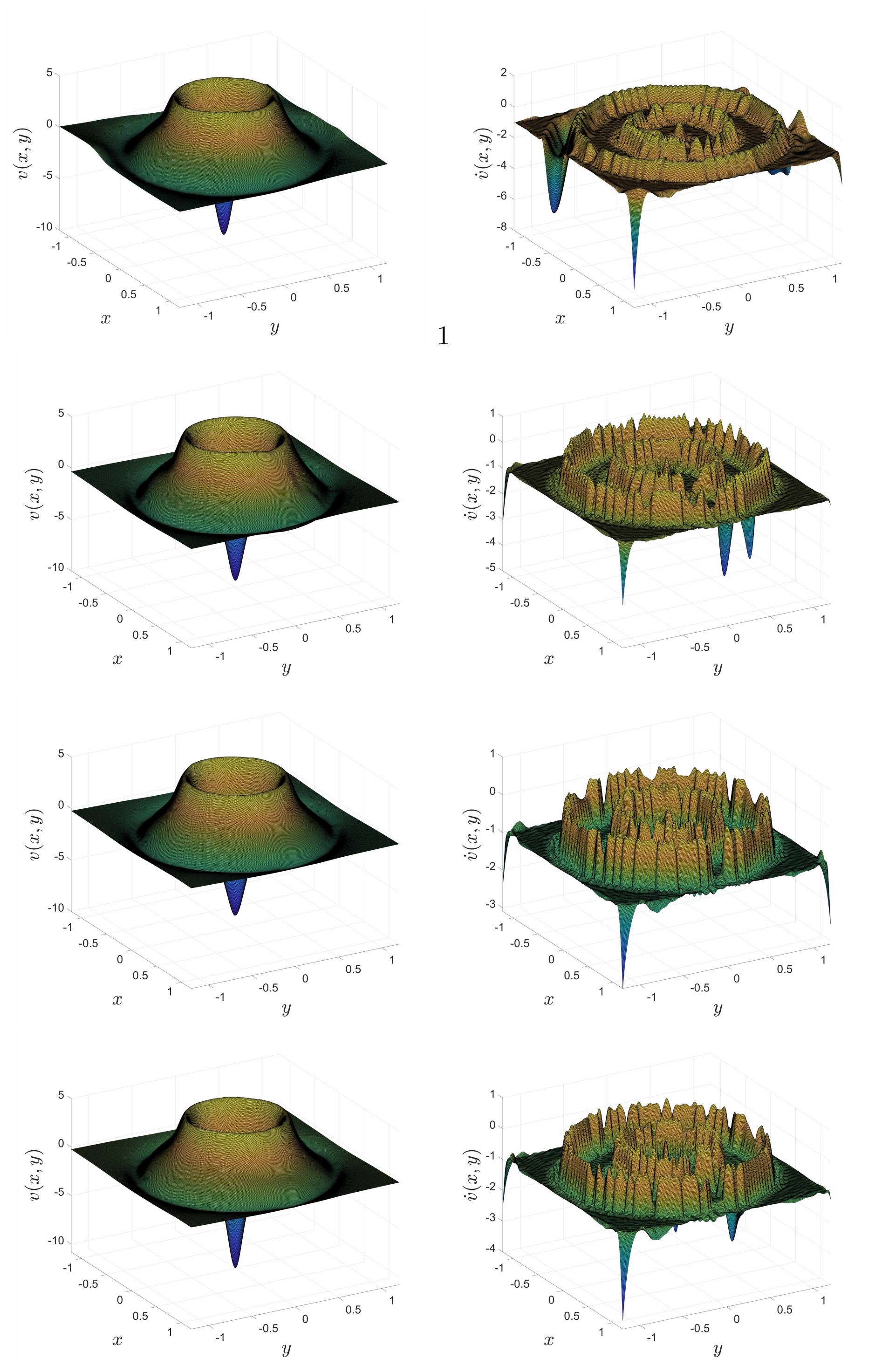

Figure 10: The CLF candidate $v(x, y)$ (left) as well as $\dot{v}(x, y)$ (right) in the second step. From top to bottom we started using the conditions $\dot{v}(x) = -1$ for $x \in I$, $x \in M$, $x \in O$, and $x \in I \cup M \cup O$ and $\dot{v}(x) \leq 0$ for the rest.

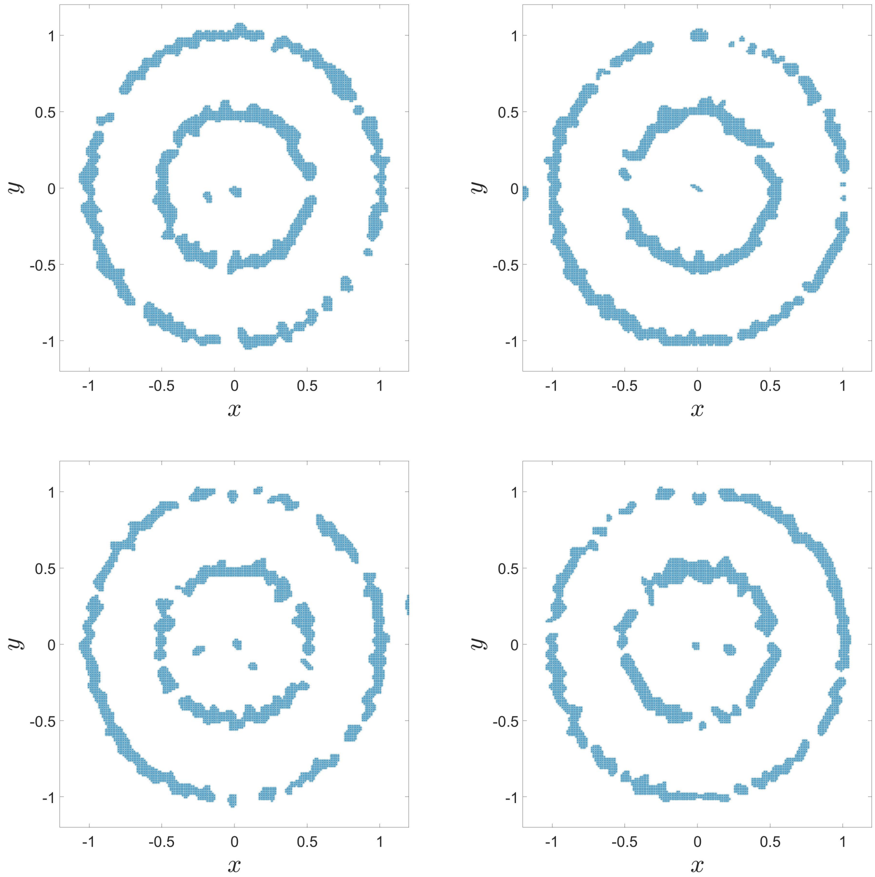

Figure 11: Second step. The area where the orbital derivative of the CPA interpolation of the computed CLF fails to have a negative orbital derivative, when using the condition $\dot{v}(x) = -1$ for $x \in I$ and $v(x) \leq 0$ for $x \in X \setminus I$ (upper left), $\dot{v}(x) = -1$ for $x \in M$ and $v(x) \leq 0$ for $x \in X \setminus M$ (upper right), $\dot{v}(x) = -1$ for $x \in O$ and $v(x) \leq 0$ for $x \in X \setminus O$ (lower left), and $\dot{v}(x) = -1$ for $x \in I \cup M \cup O$ and $v(x) \leq 0$ for $x \in X \setminus (I \cup M \cup O)$ (lower right).

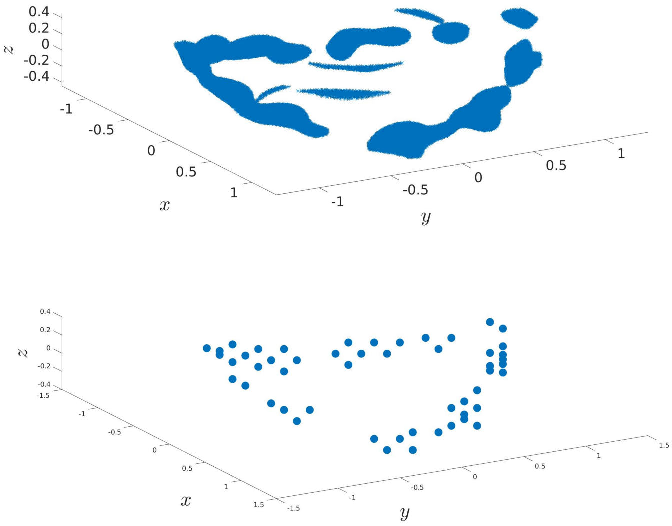

Figure 12: Second step with $\alpha = 0.18$. Top: The area in Ω where the orbital derivative of the CPA interpolation of the computed CLF fails to have a negative orbital derivative. Bottom: The collocation points x_i, such that the corresponding coefficients satisfy $\beta_i \leq -10^{-5}$. Both sets indicate the chain-recurrent set, in this case a periodic orbit. The approximation is poor due to too only 668 collocation points.

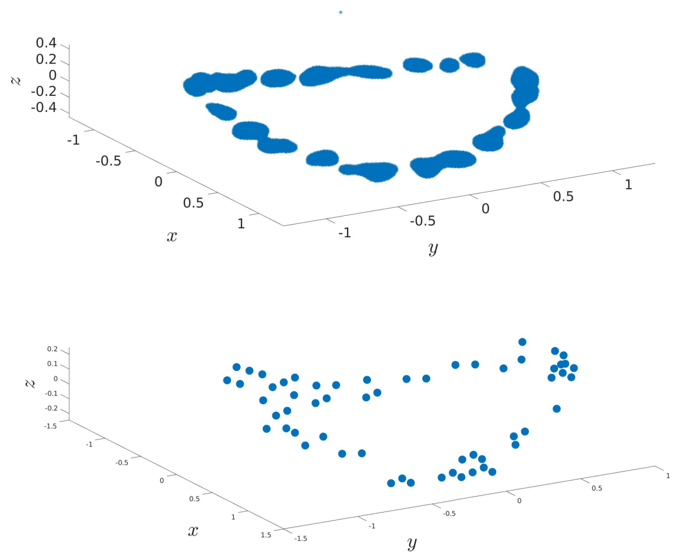

Figure 13: Second step with $\alpha = 0.12$. Top: The area in Ω where the orbital derivative of the CPA interpolation of the computed CLF fails to have a negative orbital derivative. Bottom: The collocation points x_i, such that the corresponding coefficients satisfy $\beta_i \leq -10^{-5}$. Both sets indicate the chain-recurrent set, in this case a periodic orbit. The approximation uses 2532 collocation points and is much better than with $\alpha = 0.18$ and 668 collocation points, in particular when using the orbital derivative.

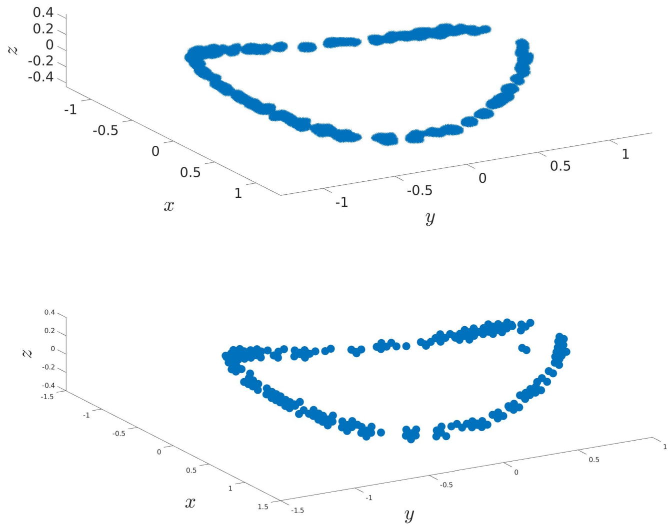

Figure 14: Second step with $\alpha = 0.06$. Top: The area in Ω where the orbital derivative of the CPA interpolation of the computed CLF fails to have a negative orbital derivative. Bottom: The collocation points x_i, such that the corresponding coefficients satisfy $\beta_i \leq -10^{-5}$. Both sets indicate the chain-recurrent set, in this case a periodic orbit. The approximation uses 18133 collocation points and is far better than with $\alpha = 0.12$ and 668 collocation points, both when using the orbital derivative and the β_i.